A MODEL OF DYNAMIC INTERACTION BETWEEN A TRAIN VEHICLE AND A RAIL TRACK

Di Mino G.
Associate Professor – University of Palermo – dimino@ing.unipa.it
Di Liberto C. M.
Ph. D. – University of Palermo – diliberto@ing.unipa.it

ABSTRACT

In recent years, high speed and heavy load technology have been the main trend in the world railway.

Some problems about the dynamic interaction and vibration of the vehicle-rail track system have also constituted a relevant research area.

The increase of the operating speed and of the heavy load involves high and higher mechanical performances of the rail track; this increase causes a dynamic stress rise that also means higher level of noise and vibrations.

In this paper it has been proposed a model of dynamic interaction between a train vehicle and a rail track.

The considered vehicle model is supported two double-axle bogies at each end and is described as a 10 degree of freedom system; the rail track as a finite long beam discretely supported at three layers of elasticity.

The dynamic interaction has been obtained by calculating the wheel-rail contact force depending on vertical irregularity function.

Such function, described as an ergodic random stationary Gauss process, has been risen from the Monte Carlo method.

As regard to the analyzed simulation cases a sensitivity analysis of model has been carried out by artificial neural network for evaluating the weight of each model input on the dynamic behaviour of the rail track.

Keywords: train-rail track interaction, ergodic Gaussian random process, neural network, sensitivity analysis.

1. INTRODUCTION

The main source of excitation of the track is represented by the vertical force determined by the wheel-rail interaction during the running of trains.

This force, even in the hypothesis of a perfect way, cannot be considered constant under the action of vertical loads, on the contrary it constitutes a system which, from the calculation and modelling point of view, is rather complex.

On the other hand, the increase of speed and of axle load which has occurred in the last years, and which still continues in many European and non-European countries, makes rise new relevant technical problems; the rise of performances required to the rail track involves a consequential increase of the dynamic stresses to whom the rail track is submitted, with negative consequences even for the noise, for the vibrations transmitted to the environment and for the running safety.

For this reason is better to underline that the study of dynamic characteristics of the rail track began only 30 years ago. Previously the dynamic effects were evaluated by means of amplifying coefficients of static loads (DAF); such coefficients, deriving from experimentations carried out on railway lines with ordinary speed, are basically running speed function, even if some surveys take into account other parameters such as the stiffness of the ground, the track conditions, the traffic and so on.

In practice, by introducing the dynamic action as the increase of the static loads, the calculation of the rail track could be made using the classical methods based on beam on elastic support. Nevertheless this method is not applicable, except in a first approximation, for all the cases which do not match the experimental conditions.

This calculation procedure is not good for the modern railway lines which must have higher performances, in relation with speed and axle load.

In this paper the authors developed a bi-dimensional model with concentrated parameters for the analysis of the dynamic interaction between a train vehicle and a rail track. The model allowed to study the dynamic behaviour of two sub-systems, evaluating the dynamic solicitation deriving from wheel-rail contact.

The validation of the model was carried out referring to the accelorometric data found by the same Authors on the railway line Alcamo-Marsala, at the km 116 (Di Mino et al 2007).

An analysis for the sensitivity of the model was finally carried out in order to evaluate the influence on the value of vibration phenomenon of some important parameters, related to rail superstructure and transport characteristics, such as: the train speed, the rail track and train type, the track conditions and the type of the ground.

2. MODEL FOR THE VERTICAL DYNAMICS OF THE TRAIN VEHICLE-RAIL TRACK SYSTEM

2.1 Dynamic equations of the train vehicle

For the train vehicle modelling we used the model shown in the figure 1. The system is made of the following elements, all modelled as rigid masses:

- the vehicle body (M_c, J_c);

– two bogies (M_t, J_t);
– four wheelsets (M_w).

The secondary suspension (K_{s2}, C_{s2}) between vehicle body and bogies, such as the primary suspension (K_{s1}, C_{s1}) between bogies and wheelsets, has been modelled by means of spring-damping elements.

The system has a 10 degrees of freedom:

– vertical translation (Z_c) and rotation of pitching (φ_c) of the vehicle body;
– vertical translation (Z_{ti} for i=1,2) and rotation of pitching (φ_{ti} for i=1,2) of the bogies;
– vertical translation of the wheels (Z_{wj} for j=1,…,4).

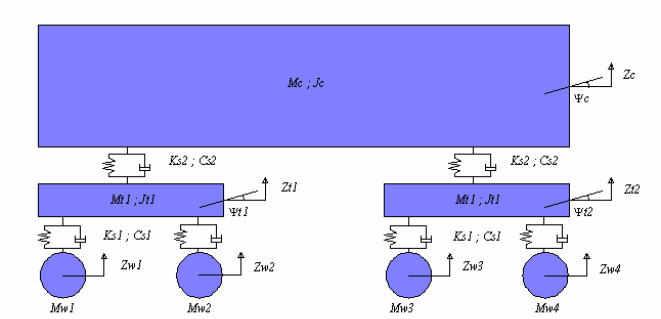

Figure 1 - Plan model of a 10 degrees of freedom train vehicle

The dynamic equation of the system is given by the relation:

$$\underline{\underline{M_v}}\,\underline{\ddot{Z}_v} + \underline{\underline{C_v}}\,\underline{\dot{Z}_v} + \underline{\underline{K_v}}\,\underline{Z_v} = \underline{F_v} \qquad \text{(Eq.1)}$$

where

$$\underline{Z_v} = \left[Z_c \quad \varphi_c \quad Z_{t1} \quad \varphi_{t1} \quad Z_{t2} \quad \varphi_{t2} \quad Z_{w1} \quad Z_{w1} \quad Z_{w1} \quad Z_{w1}\right]^T, \qquad \text{(Eq.2)}$$

$\underline{\dot{Z}_v}$ and $\underline{\ddot{Z}_v}$ are, respectively, the generalized displacement, speed and acceleration vectors, and $\underline{\underline{M_v}}$, $\underline{\underline{C_v}}$, $\underline{\underline{K_v}}$ represent the matrices of the masses, of damping and stiffness, whose expressions of $\underline{\underline{M_v}}$ e $\underline{\underline{K_v}}$, are shown as follows:

$$\underline{\underline{M_v}} = \mathrm{diag}\left[M_c \quad J_c \quad M_t \quad J_t \quad M_t \quad J_t \quad M_w \quad M_w \quad M_w \quad M_w\right]; \qquad \text{(Eq.3)}$$

$$\underline{\underline{K_v}} = \begin{bmatrix} 2K_{s2} & 0 & -K_{s2} & 0 & K_{s2} & 0 & 0 & 0 & 0 & 0 \\ & 2l_c^2K_{s2} & -l_cK_{s2} & 0 & l_cK_{s2} & 0 & 0 & 0 & 0 & 0 \\ & & 2K_{s1}+K_{s2} & 0 & 0 & 0 & -K_{s1} & -K_{s1} & 0 & 0 \\ & & & 2l_t^2K_{s1} & 0 & 0 & -l_tK_{s1} & l_tK_{s1} & 0 & 0 \\ & & & & 2K_{s1}+K_{s2} & 0 & 0 & 0 & -K_{s1} & -K_{s1} \\ & & & & & 2l_t^2K_{s1} & 0 & 0 & -l_tK_{s1} & l_tK_{s1} \\ & & & & & & K_{s1} & 0 & 0 & 0 \\ & & \text{SYMM} & & & & & K_{s1} & 0 & 0 \\ & & & & & & & & K_{s1} & 0 \\ & & & & & & & & & K_{s1} \end{bmatrix}. \quad \text{(Eq.4)}$$

The $\underline{\underline{C_v}}$ matrix is calculated substituting every elements K_{ji} of equation 4 , by C_{ji}.

The vector

$$\underline{F_v^T} = \left[-M_cg \quad 0 \quad -M_tg \quad 0 \quad -M_tg \quad 0 \quad -P_1(t) \quad -P_2(t) \quad -P_3(t) \quad -P_4(t)\right] \qquad \text{(Eq.5)}$$

represents all the loads; in this vector they are represented the time history of the wheel-rail contact forces (P_j) related to the four wheels, besides of car body, bogies and wheelsets gravity forces.

2.2 Dynamic equations of the rail track

In order to reproduce the effects created by the periodicity of the support during the running of trains, we have chosen to represent the rail track with a discrete support model; we have chosen a model used by Sato et al. (1987) and by Zhai (1992), which is characterized by 3 layers of elasticity (Fig. 2).

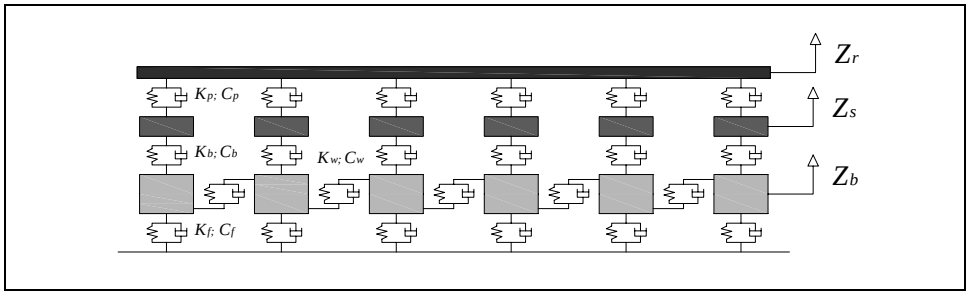

Figure 2 – Rail track model

The rail, modelled as a continuous beam, has been considered linked, with a periodicity equal to the distance of sleepers, to the rail fasteners by means of springs and dampers (K_p, C_p). These elements, representing the first level of elasticity, are linked to the lumped masses M_s, which reproduce the vertical inertia of sleepers. The

inertial behaviour of the underlying part of ballast has been modelled with the masses M_b; consequently the second level of elasticity is obtained by interposing among the concentrated masses M_s and M_b a sequence of spring-damping elements (K_b, C_b) vertically placed. Besides, in order to simulate the shear behaviour of the ballast, every mass M_b is connected to the following one by means of the K_w- C_w elements.

The K_f -C_f elements, which are bound on the upper part to the ballast elements and on the lower part to a rigid, fix base, by modelling the visco-elastic behaviour of the subgrade represent the third level of elasticity.

The rail has been modelled as a Bernoulli continuous beam (Fig. 3).

The equilibrium at the vertical lowering of the rail submitted to concentrated loads (wheel-rail contact forces) is given by the equation:

$$EI\frac{\partial^4 Z_r(x,t)}{\partial x^4} + m_r\frac{\partial^2 Z_r(x,t)}{\partial t^2} = -\sum_{i=1}^{N} F_{rsi}(t)\delta(x - x_i) + \sum_{j=1}^{N} P_j(t)\delta(x - x_{Gj}) \qquad \text{(Eq.6)}$$

where

Z_r (x, t) is the lowering of the abscissa section x at the t instant;

EI is the bending stiffness of the rail;

m_r is the mass per linear measure of the rail;

F_{rsi} is the reaction force between the rail and i^{th} sleeper;

P_j is the contact force between the rail and the j^{th} wheel;

δ_j (x) is the Dirac function;

x_i is the abscissa of the i^{th} sleeper;

x_{Gj} is the abscissa of the barycentre of the j^{th} wheel.

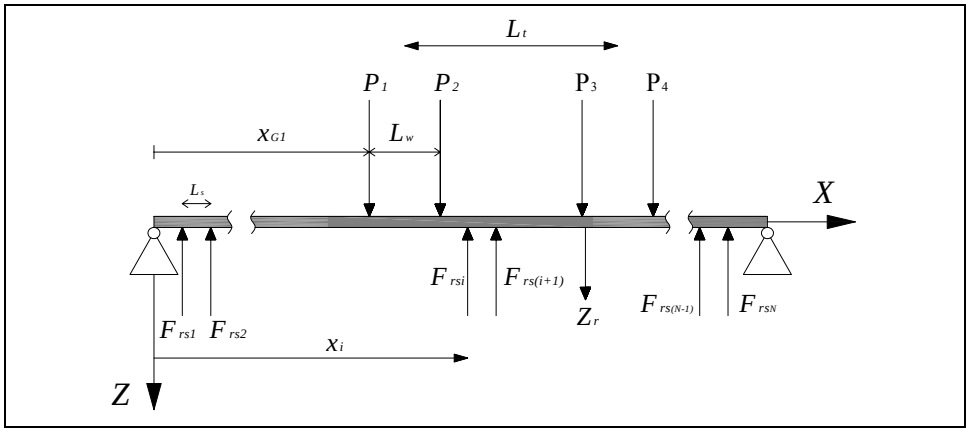

Figure 3 - Bernoulli beam model of the rail

In order to make easier to solve the equilibrium equation of the rail it is possible to use a modal approach; because the deformed shape of the rail is a "square-integrable function", the function $Z_r(x,t)$ can be obtained as superposition of K rail mode shape functions $Y_k(x)$ whose weight are given by the functions $q_k(t)$:

$$Z_r(x,t) = \sum_{k=1}^{K} Y_k(x) q_k(t) . \qquad \text{(Eq.7)}$$

The mode shape functions have the form

$$Y_k(x) = \sqrt{\frac{2}{m_r l}} \operatorname{sen} \frac{k\pi\pi}{l} \qquad \text{(Eq.8)}$$

being l the whole length of the part of the rail taken into account.

Substituting the (7) in the equilibrium equation of the rail (Eq. 6) and considering that the rail-sleeper force F_{rsi} can be determined by means of the expression

$$F_{rsi}(t) = K_{pi}[Z_r(x_i,t) - Z_{si}(t)] + C_{pi}[\dot{Z}_r(x_i,t) - \dot{Z}_{si}(t)] , \qquad \text{(Eq.9)}$$

the (6) can be expressed as follows:

$$\begin{aligned} &\ddot{q}_k(t) + \sum_{i=1}^{N} C_{pi} Y_k(x_i) \sum_{k=1}^{K} Y_k(x_i) \dot{q}_k(t) + \frac{EI}{m_r}\left(\frac{k\pi}{l}\right)^2 q_k(t) + \\ &+ \sum_{i=1}^{N} K_{pi} Y_k(x_i) \sum_{k=1}^{K} Y_k(x_i) q_k(t) - \sum_{i=1}^{N} C_{pi} Y_k(x_i) \dot{Z}_{si}(t) + \\ &- \sum_{k=1}^{K} K_{pi} Y_k(x_i) q_k(t) Z_{si}(t) = \sum_{j=1}^{4} P_j(t) Y_k(x_{Gj}) \end{aligned} \qquad \text{(Eq.10)}$$

$k = 1,2,...,K.$

Adding to the (10) the equation of motion of the sleeper and ballast elements, in matrix form we obtain:

$$\underline{\underline{M_s}}\,\underline{\ddot{Z}_s} + \underline{\underline{C_s}}\,\underline{\dot{Z}_s} + \underline{\underline{K_s}}\,\underline{Z_s} = \underline{F_s} \qquad \text{(Eq.11)}$$

which represents, in vector form (system of K+2N equations), the equation of dynamic equilibrium of the rail track. The vectors $\underline{Z_s}$, $\underline{\dot{Z}_s}$ and $\underline{\ddot{Z}_s}$ are, respectively, the generalized vectors of the displacements, of speeds, of the accelerations related to every degree of freedom of the track, $\underline{F_s}$ is the vector of the external forces, and finally $\underline{\underline{M_s}}$, $\underline{\underline{K_s}}$, $\underline{\underline{C_s}}$ represent, respectively the matrices of masses, stiffness and dissipation:

$$\underline{Z_s} = \left[q_1 \quad \cdots \quad q_K \quad Z_{s1} \quad \cdots \quad Z_{sN} \quad Z_{b1} \quad \cdots \quad Z_{bN}\right]^T ; \qquad \text{(Eq.12)}$$

$$\underline{F_s} = \left[\sum_{j=1}^{4} P_j Y_1(x_{Gj}) \quad \cdots \quad \sum_{j=1}^{4} P_j Y_K(x_{Gj}) \quad M_{s1} \cdot g \quad \cdots \quad M_{sN} \cdot g \quad M_{b1} \cdot g \quad \cdots \quad M_{bN} \cdot g \right]^T; \tag{Eq.13}$$

$$\underline{\underline{M_s}} = \begin{bmatrix} \underline{\underline{I}}_{KxK} & \underline{\underline{0}}_{NxK} & \underline{\underline{0}}_{NxK} \\ \underline{\underline{0}}_{KxN} & \begin{bmatrix} M_{s1} & & \\ & \ddots & \\ & & M_{sN} \end{bmatrix} & \underline{\underline{0}}_{NxN} \\ \underline{\underline{0}}_{KxN} & \underline{\underline{0}}_{NxN} & \begin{bmatrix} M_{b1} & & \\ & \ddots & \\ & & M_{bN} \end{bmatrix} \end{bmatrix}; \tag{Eq.14}$$

$$\underline{\underline{K_s}} = \begin{bmatrix} \underline{\underline{A}}_{KxK} & B_{NxK} & \underline{\underline{0}}_{NxK} \\ \underline{\underline{C}}_{KxN} & \underline{\underline{D}}_{NxN} & \begin{bmatrix} -K_{b1} & & \\ & \ddots & \\ & & -K_{bN} \end{bmatrix} \\ \underline{\underline{0}}_{KxN} & \begin{bmatrix} -K_{b1} & & \\ & \ddots & \\ & & -K_{bN} \end{bmatrix} & \underline{\underline{E}}_{KxN} \end{bmatrix}; \tag{Eq.15}$$

$$\underline{\underline{C_s}} = \begin{bmatrix} \underline{\underline{\hat{A}}}_{KxK} & \hat{B}_{NxK} & \underline{\underline{0}}_{NxK} \\ \underline{\underline{\hat{C}}}_{KxN} & \underline{\underline{\hat{D}}}_{NxN} & \begin{bmatrix} -C_{b1} & & \\ & \ddots & \\ & & -C_{bN} \end{bmatrix} \\ \underline{\underline{0}}_{KxN} & \begin{bmatrix} -C_{b1} & & \\ & \ddots & \\ & & -C_{bN} \end{bmatrix} & \underline{\underline{\hat{E}}}_{KxN} \end{bmatrix}; \tag{Eq.16}$$

where

$$\underline{\underline{A}}_{KxK} = \begin{bmatrix} \frac{EI}{m_r}\left(\frac{\pi}{l}\right)^4 + \sum_{i=1}^{N} K_{pi} Y_1^2(x_i) & \sum_{i=1}^{N} K_{pi} Y_1(x_i) Y_2(x_i) & \cdots & \sum_{i=1}^{N} K_{pi} Y_1(x_i) Y_K(x_i) \\ & \frac{EI}{m_r}\left(\frac{2\pi}{l}\right)^4 + \sum_{i=1}^{N} K_{pi} Y_2^2(x_i) & & \vdots \\ & & \ddots & \\ \text{Symm} & & & \frac{EI}{m_r}\left(\frac{K\pi}{l}\right)^4 + \sum_{i=1}^{N} K_{pi} Y_K^2(x_i) \end{bmatrix}, \quad \text{(Eq.17)}$$

$$\underline{\underline{B}}_{NxK} = \begin{bmatrix} -K_{p1} Y_1(x_1) & -K_{p2} Y_1(x_2) & \cdots & -K_{pN} Y_1(x_N) \\ -K_{p1} Y_2(x_1) & -K_{p2} Y_2(x_2) & \cdots & -K_{pN} Y_2(x_N) \\ \vdots & \vdots & \ddots & \vdots \\ -K_{p1} Y_K(x_1) & -K_{p2} Y_K(x_2) & & -K_{pN} Y_N(x_N) \end{bmatrix}, \quad \text{(Eq.18)}$$

$$\underline{\underline{C}}_{KxN} = \begin{bmatrix} -K_{p1} Y_1(x_1) & -K_{p1} Y_1(x_1) & \cdots & -K_{p1} Y_K(x_1) \\ -K_{p2} Y_1(x_2) & -K_{p2} Y_2(x_2) & \cdots & -K_{p2} Y_K(x_2) \\ \vdots & \vdots & \ddots & \vdots \\ -K_{pN} Y_1(x_N) & -K_{pN} Y_2(x_N) & & -K_{pN} Y_K(x_N) \end{bmatrix}, \quad \text{(Eq.19)}$$

$$\underline{\underline{D}}_{NxN} = \begin{bmatrix} K_{p1} + K_{b1} & 0 & \cdots & 0 \\ 0 & K_{p2} + K_{b2} & \cdots & 0 \\ \vdots & \vdots & \ddots & \vdots \\ 0 & 0 & & K_{pN} + K_{bN} \end{bmatrix}, \quad \text{(Eq.20)}$$

$$\underline{\underline{E}}_{NxN} = \begin{bmatrix} \begin{pmatrix} K_{b1} + K_{f1} + \\ + K_{w1} \end{pmatrix} & -K_{w1} & 0 & \cdots & 0 \\ -K_{w1} & \begin{pmatrix} K_{b2} + K_{f2} + \\ + K_{w2} \end{pmatrix} & -K_{w2} & \cdots & 0 \\ 0 & -K_{w2} & \begin{pmatrix} K_{b3} + K_{f3} + \\ + K_{w3} \end{pmatrix} & \ddots & 0 \\ \vdots & \vdots & \ddots & \ddots & -K_{wN} \\ 0 & 0 & 0 & -K_{wN} & \begin{pmatrix} K_{bN} + K_{fN} + \\ + K_{wN} \end{pmatrix} \end{bmatrix}; \quad \text{(Eq.21)}$$

the matrices $\hat{\underline{\underline{A}}}_{KxK}$, $\hat{\underline{\underline{B}}}_{NxK}$, $\hat{\underline{\underline{C}}}_{KxN}$, $\hat{\underline{\underline{D}}}_{NxN}$, $\hat{\underline{\underline{E}}}_{NxN}$ can be obtained from the homonymous only changing K_{ji} in C_{ji}.

2.3 Train vehicle-track interaction

Assembling into one relation the equations (1) and (11) the global equilibrium equation of the system train vehicle-track is obtained:

$$\underline{\underline{M}}\ddot{\underline{Z}} + \underline{\underline{C}}\dot{\underline{Z}} + \underline{\underline{K}}\underline{Z} = \underline{F} \qquad \text{(Eq.22)}$$

where $\underline{Z}$, $\dot{\underline{Z}}$ e $\ddot{\underline{Z}}$ are, respectively, the generalized displacements, speeds and accelerations vectors, $\underline{F}$ is the vector of external forces, and $\underline{\underline{M_s}}$, $\underline{\underline{K_s}}$, $\underline{\underline{C_s}}$ represent respectively the matrices of the masses, rigidity and dissipation:

$$\underline{Z} = \begin{bmatrix} \underline{Z_v} \\ \underline{Z_s} \end{bmatrix}; \qquad \dot{\underline{Z}} = \begin{bmatrix} \dot{\underline{Z}}_v \\ \dot{\underline{Z}}_s \end{bmatrix}; \qquad \ddot{\underline{Z}} = \begin{bmatrix} \ddot{\underline{Z}}_v \\ \ddot{\underline{Z}}_s \end{bmatrix}; \qquad \underline{F} = \begin{bmatrix} \underline{F_v} \\ \underline{F_s} \end{bmatrix};$$

$$\underline{\underline{M}} = \begin{bmatrix} \underline{\underline{M_v}} \\ \underline{\underline{M_s}} \end{bmatrix}; \qquad \underline{\underline{K}} = \begin{bmatrix} \underline{\underline{K_v}} \\ \underline{\underline{K_s}} \end{bmatrix}; \qquad \underline{\underline{C}} = \begin{bmatrix} \underline{\underline{C_v}} \\ \underline{\underline{C_s}} \end{bmatrix}. \qquad \text{(Eq.23)}$$

The vector $\underline{F}$ contains the terms $P_j(t)$, which can be calculated using the Hertz contact theory. If, hypothetically, the track presents vertical irregularities, whose longitudinal trend is given by the function $Z_0(x)$, the wheel-rail contact force can be determined by means of the relation (Fig.4):

$$P_j(t) = C_H \cdot \left[Z_{wj}(t) - Z_r(x_{Gj}, t) - Z_0(Vt) \right]^{3/2} \qquad j = 1,...,4 \qquad \text{(Eq.24)}$$

where C_H is the "coefficient of Hertz contact", $Z_{wj}(t)$ is the lowering of the j^{th} wheel at the t instant, and $Z_r(x_{Gj,}t)$ is the lowering that the rail has at the t instant at the point of contact with j^{th} wheel.

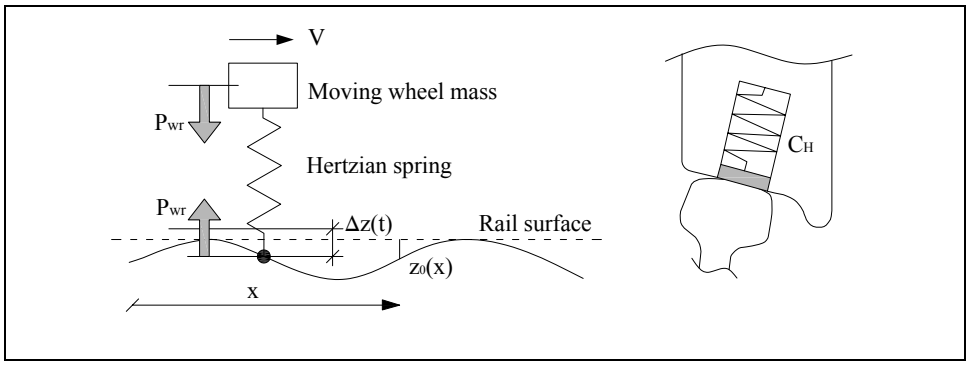

Figure 4 - Hertz contact model for the wheel-rail interaction.

The quantity $\Delta Z(t) = Z_w(t) - Z_r(x,t) - Z_0(Vt)$ represents the vertical deformation of the wheel-rail contact.

The coefficient C_H has been determined by means of the expression (Sun Y.Q. et al. 2002):

$$C_H = \frac{4G_{wr}\sqrt{R_e}}{3(1-\nu_{wr})} \qquad \text{(Eq.25)}$$

where G_{wr} is the shear modulus, ν_{wr} is the Poisson's ratio; R_e is given by the relation:

$$R_e = \sqrt{r\left(\frac{\rho_w R_t}{\rho_w - r}\right)} \qquad \text{(Eq.26)}$$

where r is the rolling radius of the wheel, ρ_w is the wheel profile radius and R_t is the rail profile radius.

The defect $Z_0(x)$ of the track can be considered as an stationary ergodic Gauss random process with expectation zero (Roberts B.J. et al. 1990).

Indicating with $S_z(\Omega)$ the power spectral density of the vertical irregularity, the r^{th} sample of the process is obtained by means of the relation (Muscolino G. 2002):

$$z_0^{(r)}(x) = \sum_{k=1}^{N} \sqrt{2 \cdot S_z(\Omega_k)\Delta\Omega} \cdot \text{sen}(\Omega_k x + \varphi_k^{(r)}) \qquad \text{(Eq.27)}$$

where $\varphi_k^{(r)}$ is a random variable with a constant density of probability (equal to $1/2\pi$) in the range $[0, 2\pi]$, and Ω is the space angular frequency.

The quantity $\Delta\Omega$ represents the sampling range of the $S_z(\Omega)$, so that, by indicating with Ω_{sup} and Ω_{inf} the upper and lower extremes of the range of Ω taken into account, the Ω_k is:

$$\Omega_k = \Omega_{inf} + \left(k - \frac{1}{2}\right)\Delta\Omega \qquad \text{(Eq.28)}$$

with $\Delta\Omega = (\Omega_{sup} - \Omega_{inf})/2$.

The variables $\varphi_k^{(r)}$ are independent the one from the other and they were risen from the Monte Carlo method.

The relation (28) allows to arise numerically the space trend of the vertical irregularities, once known the relative PSD. To evaluate the vertical defect of the track the spectrums found in technical publications can be used. (Lei X. et al. 2002, Panagin R. 1990).

The step by step integration of the equation (23) was made by means of the Newmark-β method.

In order to take into account the monolateral constraint of the wheel-rail contact, a practice of control on the $\Delta Z_j(z)$ was developed, in order that $P_j(t)=0$ when, at the generic t instant, it resulted $\Delta Z_j(z)<0$ (detachment condition)

2.4 Demonstration of the model

The model was applied to a section of the railway line Alcamo-Marsala (116 km), in this site a series of accelerometric assays on the track was carried out (Di Mino et al. 2007). The site is characterized by a track with ballast, wooden sleeper and K-fastener.

The model was realized taken into account a one hundred sleeper railway section, 64.35 m long.

As for the rail, the first 200 vibration ways were considered, so that the system has a total of 410 degrees of freedom.

In order to validate the model we considered the running of a ALn 688 train with a single configuration, having a 90km/h speed, whose mechanical parameters are shown in table 1.

Table 1 - Characteristic parameters of the ALn 688 train

Car body mass [kg]	28800
Bogie mass [kg]	3600
Wheelset mass [kg]	500
Total length [mm]	23540
Wheel distance [mm]	2450
Bogie distance [mm]	15950
Primary suspension stiffness [kN/m]	5×10^5
Secondary suspension stiffness [kN/m]	$8{,}8\times10^5$
Primary suspension damping [N s/m]	500
Secondary suspension damping [N s/m]	41500

The values of the parameters used for modelling the track are shown in table 2.

Table 2 - Characteristic parameters of the track

m_r **[kg/m]**	50	l **[m]**	64,35
EI **[N m^2]**	3872400	l_s **[m]**	0,65
M_s **[kg]**	33	M_b **[kg]**	700
K_b **[N/m]**	240×10^6	C_b **[N sec/m]**	$58{,}8\times10^3$
K_p **[N/m]**	265×10^6	C_p **[N sec/m]**	40×10^3
K_f **[N/m]**	$76{,}85\times10^6$	C_f **[N sec/m]**	$64{,}6\times10^3$
K_w **[N/m]**	$78{,}4\times10^6$	C_w **[N sec/m]**	80×10^3

The irregularity of the track was calculated using the PSD proposed by the America Railway Standard for the 6 class railway lines (Lei X. et al. 2002).

In order to reduce the most the boundary effects, the response of the system was calculated in the central point of the model.

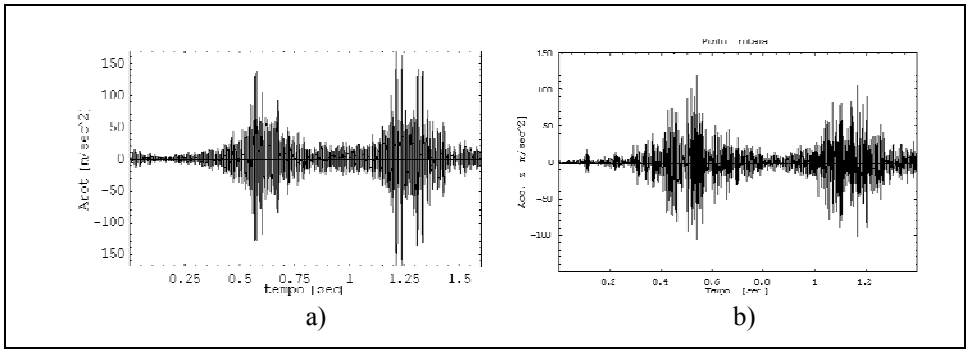

Figure 5 – Vertical acceleration of the rail: a) numerical; b) experimental

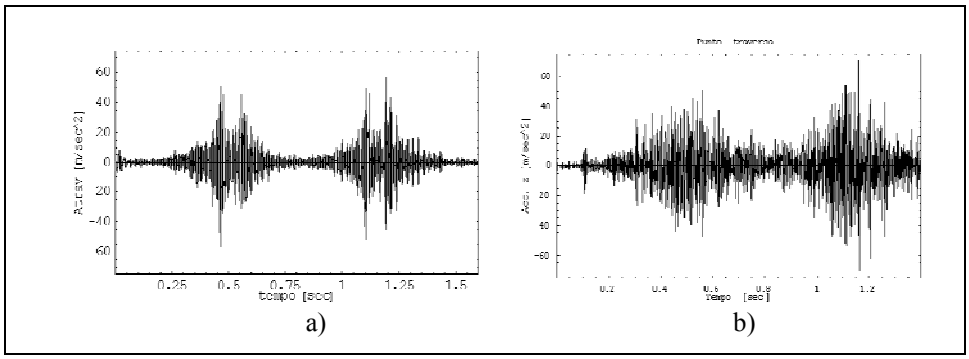

Figure 6 – Vertical acceleration of the sleeper: a) numerical; b) experimental

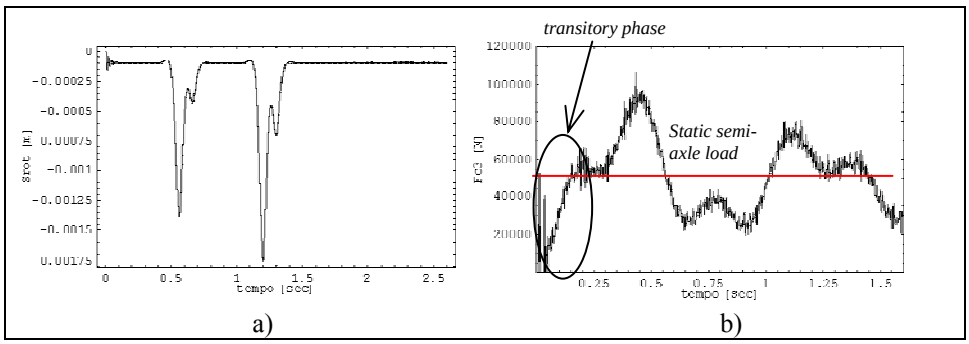

Figure 7 – a) Vertical displacement of the rail b) Wheel- rail contact force

The numerical results were compared with the accelerometric data gathered directly on site on the rail and on the sleeper.

In figure 5 the time history of the vertical acceleration of the rail are shown, respectively numerical and experimental; there is a good accordance between the

numerical and experimental data. The same can be said as for the vertical acceleration of the sleeper (Fig. 6).

The vertical displacement numerically calculated of the rail is shown in the figure 7-a; the top range of the displacement is in accordance with the data found in technical publications in the same conditions (Accattatis F. et al.1991, Cioffi E. et al. 2003).

Figure 7-b shows the time history of the wheel-rail contact force, which was numerically calculated; the transitory phase, lasting about 0.2 sec., is due to the imposition of initial null conditions.

3. SENSITIVITY ANALYSIS OF THE TRAIN VEHICLE-RAIL TRACK SYSTEM BY NEURAL NETWORKS

Among the different causes which are involved in the dynamic interaction between the two systems train vehicle-rail track, the following factors were identified:

- running speed of the train;
- type of the train;
- type of the rail track;
- type of the ground;
- track conditions.

The sensitivity analysis of the system was carried out planning different cases obtained by changing the values related to the above mentioned factors.

3.1 The analysis on the simulated cases

The analysis was carried out taking into account four running speeds of trains: 54 km/h, 72 km/h, 108 km/h and 144 km/h.

Table 3 - Characteristic parameters of the considered trains

Train	***C62A***	***ETR500***
M_c **[kg]**	77000	29670
M_t **[kg]**	1100	6250
M_w **[kg]**	1200	1580
J_c **[kg m^2]**	1200000	1824000
J_t **[kg m^2]**	760	2500
K_{s1} **[N/m]**	2140000	1617500
C_{s1} **[N s/m]**	49000	1470
K_{s2} **[N/m]**	5320000	722200
C_{s2} **[N s/m]**	70000	63800

In order to consider the incidence of the vehicle factor on the response of the system, two types of locomotives were considered: the C62A type, which runs on the main Chinese railway lines, and the lighter ETR 500 type of the Italian National Railways (FS) (Tab. 3).

Two track options were taken into account: we modelled the track with ballast, concrete sleeper and rail of the UIC60 type, which was considered as it was equipped in one case with a rigid fastener and in the other case with an elastic fastener (table 4).

The influence of the geotechnical characteristics was evaluated taken into account two types of ground (Tab. 4).

Table 4 - Characteristic parameters of the rail track and the ground

RAIL TRACK	l [m]	30	EI [N m^2]	6145500
	l_s [m]	0,6	m_r [kg/m]	60
	M_s [kg]	250	K_b [N/m]	240×10^6
	M_b [kg]	700	C_b [N s/m]	$58{,}80\times10^3$
	K_w [N/m]	$78{,}40\times10^6$	C_w [N sec/m]	80×10^3
	Rigid fastener		**Elastic fastener**	
	K_p [N/m]	1000×10^6	K_p [N/m]	$100{,}42\times10^6$
	C_p [N s/m]	100×10^3	C_p [N s/m]	12000×10^3
GROUND	**Sand**		**Clay**	
	K_f [N/m]	230×10^6	K_f [N/m]	$76{,}85\times10^6$
	C_f [N s/m]	$48{,}52\times10^3$	C_f [N s/m]	$64{,}60\times10^3$

The rail track conditions were considered making reference to the vertical irregularity of the track. Two types of irregularities were taken into account: in one case we used the spectrum given by the SNCF on the assays made between the km 136 and 137 of high speed railway line Paris-Toulouse, in the other case we referred to the spectrum given by the America Railway Standard for the ordinary speed railway.

The simulation study was carried out by modelling 64 different settings obtained by combining together all the above mentioned parameters.

For each setting we determined the time history of the cinematic response of the train vehicle-rail track system, and also the time history of the forces of wheel-rail and rail-sleeper contact. The greatest values of the above mentioned quantities during the time range of calculation were determined.

3.2 Process of neural elaboration

The use of neural networks allows to evaluate the contribution related to each factor, observed while it participates together with the others to determine the dynamic phenomenon.

The speed of the train (V), the damping (C_p) and the stiffness of the fastener (K_p), the mass of the vehicle (M_v) and the stiffness of the vehicle suspension (K_{s2}), the stiffness (K_f) and the damping (C_f) of the ground, and the type of irregularity of the track (Irr) are the input data (cause) to put in the network.

Six parallel elaborations were carried out, putting as output data the displacement (Z_w) and the acceleration (A_w) of the wheel, the wheel-rail contact force (P_{wr}), the displacement (Z_r) and the acceleration of the rail (A_r), the rail-sleeper contact force (F_{rs}).

Both the input and the output data were normalized with reference to the corresponding greatest value.

The implementation of a neural network requires some fundamental actions, such as the choice of its structure and the definition of the parameters which are typical of the training process and of the relative characteristic values.

The method, concerning the network structure, consisting in changing the number of both the hidden layers and the related nodes, generally allows to have satisfying and reliable results, also according to the extent of the range of configurations taken into account.

Table 5 – Network elements and training parameters

NETWORK STRUCTURE	
Input nodes	6
Output nodes	1
Nodes in the hidden layers	5 ÷ 9
Network layers	3 ÷ 5
Hidden layers	1 ÷ 3
TRAINING PARAMETER	
Iteration	100000 ÷ 200000
Momentum factor	0,8
Learning rate	0,01÷0,1
Training set cases	58
Test set cases	10% training set
Selection process of test cases	random
Transfer function	Sigmoid

The data sets of input and output were put in adequate files in order to be acquired and processed directly by the neural network system we choose BPNN (Back Propagation Neural Network) with exclusive forward transmission of the signal.

The phases of training and test of the information put in the network, which are the elaboration and learning processes, are given by the number of the iterations, by the type of transfer function, by the learning rate and by the moment.

In this case, the fields of variations of the parameters related to the project of the network architecture and to the training process are shown in table 5.

Table 6 - Network elements and training parameters

ADMISSIBILITY RANGES	
Training set RMS error	0,02 ÷ 0,10
Test set RMS error	0,02 ÷ 0,12
Training set Correlation	0,5 ÷ 1,00
Test set Correlation	0,5 ÷ 1,00

Rather than determine the network architecture, more appropriate to analyse the problem, by means of a heuristic procedure, whose result depends on the number of

tests made, not assuring the univocity of the solution, we preferred another type of procedure. Sixty networks were trained, among them we choose only the networks, which in terms of root mean square of the error and in terms of correlation coefficient, during the training and test phases, showed at the end of the iterative procedure values which are included in the admissibility range shown in the table 6.

According to this choice the significant networks were the 42% of the total.

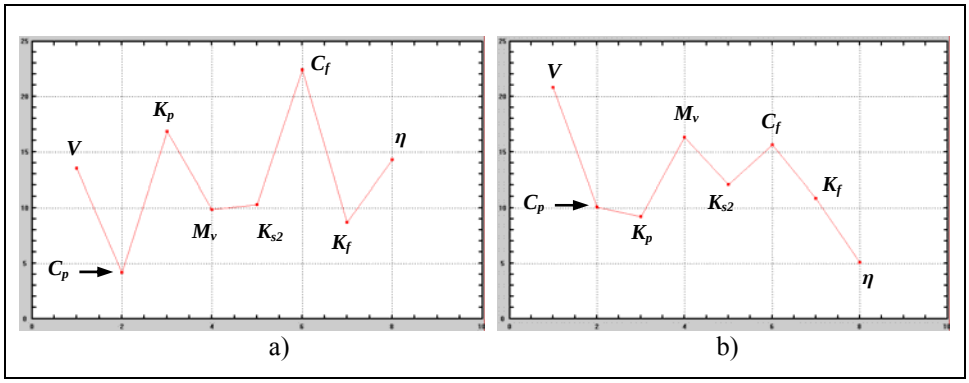

Figure 8 – Diagram of the percent contribution: a) case of the acceleration of the rail; b) case of the wheel-rail contact force

At the end of the elaboration the neural network gives the diagrams of the related hierarchy, of which two examples are shown in figure 8, respectively for the acceleration of the rail and for the wheel-rail contact force, remembering that these hierarchies are significant only when the considered parameters act at the same time.

In order to identify the most reliable hierarchy of contribution, the interpretation of results, obtained from the significant networks, was made by means of the *Method of the recurrence* (Di Mino G. et al. 2005). The criterion lies in selecting the most recurrent sequence of the inputs, arranged according to weight; the values of the contribution of each one are the average values given by this more restricted sample.

The analysis results are shown in figures 9, 10 and 11.

3.3 Analysis of the results

As for the displacement of the wheel (Fig. 9-a) and of the rail (Fig. 9-b), hierarchies of the weight of inputs influence are found, which are almost coincident: the fundamental contribution is given by the stiffness of the fastener and of the ground, with the latter having a lightly lower weight. Stiffness of the suspensions, vehicle mass and irregularity give, in this order, the lower contributions, while the damping of the ground and of the fastener, and the speed represent considerable contributions, which are almost comparable.

As for the wheel and rail acceleration (Fig. 10) the most influencing factor is the speed: nevertheless as for the rail the influence is higher.

Referring to the wheel acceleration (Fig. 10-a) the damping of the ground, the vehicle mass, the stiffness of the fastener, of the suspensions and of the ground give, in

this order, comparable contributions, having values of the related weights which are included in the range 11-17%. The damping of the fastener and the irregularity give the lowest contributions, and the first parameter has a lightly higher value.

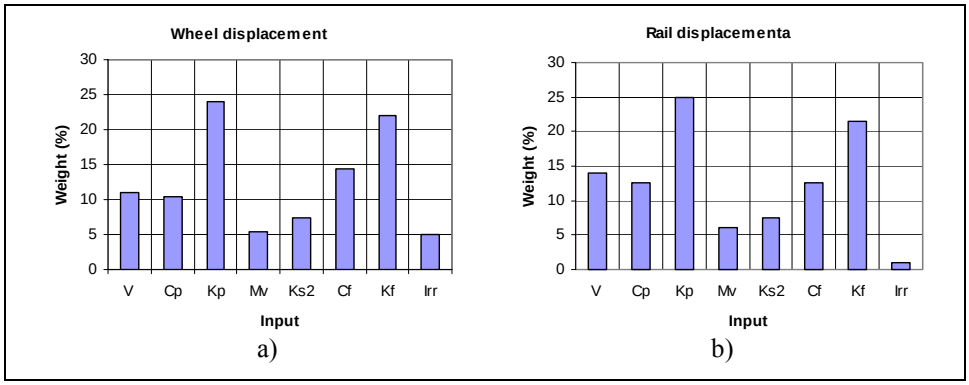

Figure 9 – Results of the analysis: a) wheel displacement; b) rail displacement

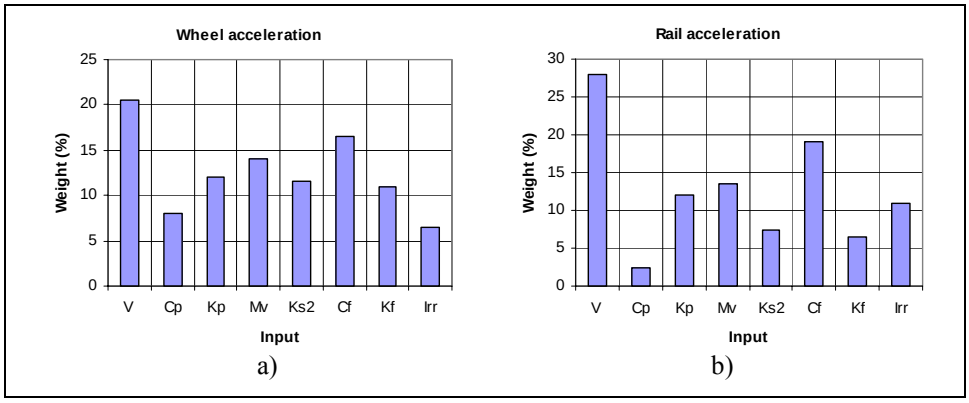

Figure 10 – Results of the analysis: a) wheel acceleration; b) rail acceleration

As for the rail acceleration (Fig.10-b) the damping of the ground, after the speed, gives the most significant contributions (19%). Vehicle mass, stiffness of the fastener and irregularity give, in this order, comparable weights, even if they are lightly different (16-19%). Stiffness of the suspensions and of the ground are at about 17%, while the lowest contribution is the one given by the stiffness of the fastener.

With reference to the contact forces (Fig. 11), the speed still has the greater weight, having an incidence of 21% as for the P_{wr} and of 33% as for the F_{rs}.

As for the wheel-rail contact force (Fig. 11-a), the vehicle mass and the damping of the ground give the same influence (16%); stiffness of the suspensions and of the ground, damping and rigidity of the fastener have almost similar contribution, having values of the related weights which are included between 9% and 16%. The lowest contribution, in this case, is the one of the irregularity (5%).

Concerning the rail-sleeper contact force (Fig. 11-b), the gap between the contribution given by the speed and the one given by the other parameters is more evident: damping of the ground, vehicle mass, damping of the fastener and stiffness of the suspensions have, in this order, weight values which are included between 10% and 15%, while the rigidity of the fastener, the irregularity and the rigidity of the ground keep having, in this order, values which are lightly higher than 5%.

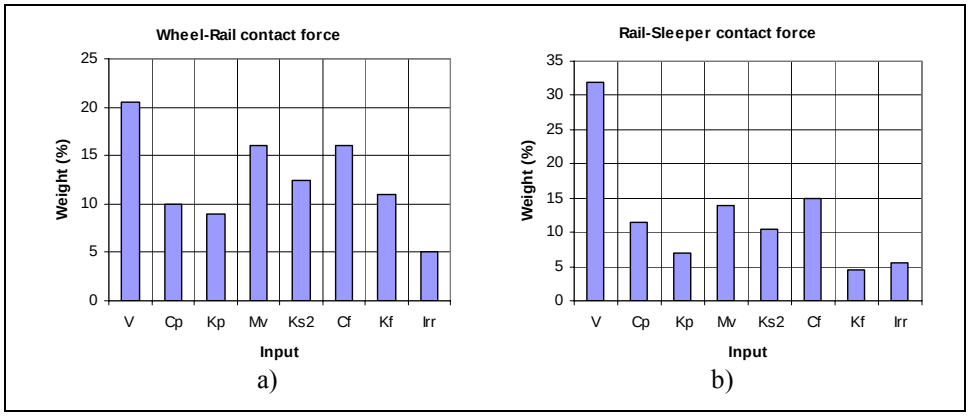

Figure 11 – Results of the analysis: a) wheel-rail contact force; b) rail-sleeper contact force

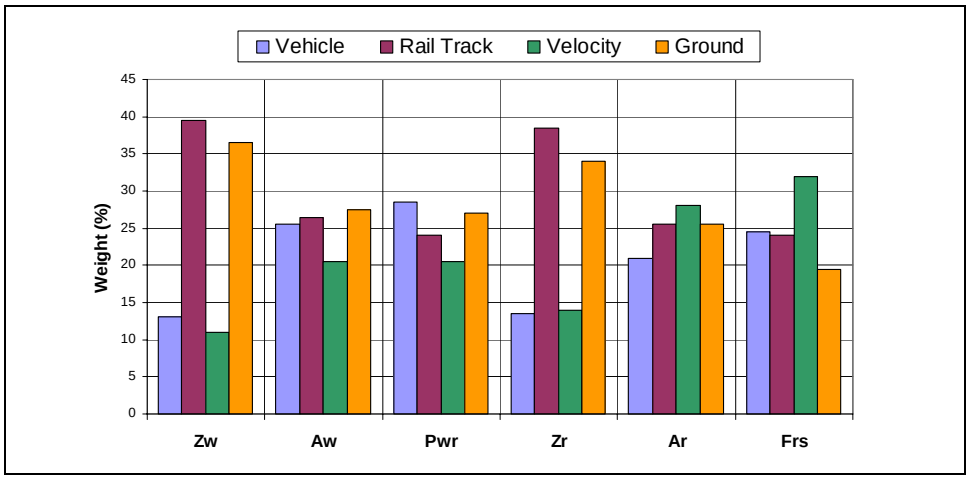

Figure 12 – Influence of the elements of the rail system on the outputs

In order to stress the total influence on the response of the system, respectively of the vehicle, the rail track, the speed and the ground, we aggregated the weights of the related ranges of inputs.

The result is shown in figure 12: it can be seen that, in an aggregated form, the rail track and the ground play a prevailing role in the generation and propagation of the dynamic phenomena.

4. CONCLUSIONS

The problems related to the vertical loads are very considered in the management and maintenance of railway systems.

A complex bi-dimensional model, gauged by means of experimental results, can be very useful as mean of preliminary calculation of cinematic and mechanical data which lead to management and economic evaluations of railway systems.

The main peculiarity of the proposed model is to consider from a stochastic point of view the track irregularities, which vertically imply dynamic overloads and displacements which must be carefully determined and checked.

Finally, through the sensitivity analysis carried out by means of Artificial Neural Network on a range of technical, realistic cases, which were simulated changing opportunely the system elements, what comes out significantly is that the rail track and the ground contribute in a prevailing way, whatever are their nature or type, to enhance the cinematic and dynamic phenomena, which cause well known problems such as vibrations.

Once chosen to face extended cases of modelling including even the analysis of the grounds, from what said previously it derives the necessity to pay particular attention to the dynamic modelling of the ground, and moreover the necessity of an exact modelling of the secondary elements of the rail track (fasteners) which greatly influence the mechanical behaviour of the system on its whole.

REFERENCES

ACCATTATIS, F., COLLETTI, G., CORRIDORI, A., MALAVASI, G. (1991) – *"Le vibrazioni dell'armamento ferroviario: considerazioni teoriche e verifiche sperimentali" – Ingegneria Ferroviaria*, maggio, pp. 285-303.

BEVILACQUA, A., DI MINO, G., GIUNTA, M. (1999) – "*L'analisi della fase applicativa di architettura di rete neurale per lo studio del fenomeno dell'incidentalità autostradale*" – Quarry and Construction, XXXVII, 4, pp.130-136.

CIOFFI, E., CORAZZA, R., KAJON, G. (2003) – *"Caratteristiche e prestazioni degli armamenti" – Ingegneria Ferroviaria*, febbraio, pp. 121-133.

DI MINO, G., NIGRELLI, J., RODONO', G. (2005) – *"Indagine sperimentale per la valutazione del confort acustico nei vagoni ferroviari" – Ingegneria Ferroviaria*, gennaio, pp. 45-54.

DI MINO, G., DI LIBERTO, C. M., NIGRELLI, J. (2007) – *"A FEM model of rail track-ground system to calculate the ground borne vibrations: a case of rail track with wooden sleepers and k-fastenings at Castelvetrano" – Advanced Characterisation of Pavement and Soil Engineering Materials*, 20-22 June, Athens, Greece.

LEI, X., NODA, N.-A. (2002) – *"Analyses of dynamic response of vehicle and track coupling system with random irregularity of track vertical profile" – Journal of Sound and Vibration*, 258, 1, pp. 147-165.

MUSCOLINO G. (2002) – *"Dinamica delle strutture"* – McGraw-Hill, Milano.

PANAGIN R. (1990) – *"La dinamica del veicolo ferroviario"* – Levrotto e Bella, Torino.
ROBERTS, J. B., SPANOS, P.D. (1990) – *"Random Vibration and Statistical Linearization"* – John Wiley & Sons Ltd, New York.
SATO, Y., ODAKA, T. and TAKAI, H. (1987) – *"Theoretical analysis on vibration of ballasted track" – Railway Technical Research Report* No. 1347.
SUN, Y.Q., DHANASEKAR, M. (2002) – *"A dynamic model for the vertical interaction of the rail track and wagon system" – International Journal of Solids and Structures*, 39,1337-1359.
ZHAI, W. (1992) – "The vertical model of vehicle-track system and its coupling dynamics" – *J. of the China Railway Society*, 14, 3, pp. 21-29.